Performance Analysis of Space–Time Line Code Systems with Phase-Shift Keying Modulation

Chan Hyung Kim, Yojin Lim, Seung-Chan Lim[*], and Jingon Joung[†]
School of Electrical, Electronic and Control Engineering, Hankyong National University, Anseong, South Korea
[*]School of ICT, Robotics and Mechanical Engineering and IITC, Hankyong National University, Anseong, South Korea
[†]School of Electrical and Electronics Engineering, Chung-Ang University, Seoul, South Korea
{cksguddl841, dywls605}@hknu.ac.kr, sclim@hknu.ac.kr[†], jgjoung@cau.ac.kr[*]

***Abstract*—The performance of space–time line code (STLC) systems employing phase-shift keying (PSK) modulation has not been studied, despite the distinct advantage of eliminating the need to estimate partial channel state information at the receiver. In this study, we comprehensively analyze the fundamental performance of STLC systems when utilizing PSK modulation, focusing on three essential aspects: 1) symbol error rate, 2) bit error rate, and 3) diversity gain and coding gain. The mathematical analysis is rigorously validated through numerical simulations, revealing system performance behavior concerning modulation order and the number of transmit antennas.**

***Index Terms*—Coding gain, diversity gain, error rate, phase-shift keying, space–time line code.**

I. Introduction

Recently, the space–time line code (STLC) has garnered substantial attention in various multiple-antenna systems with full channel state information (CSI) at the transmitter (CSIT) and partial CSI at the receiver (CSIR) [1]. Exploiting the inherent advantages, the STLC has exhibited the capability to improve the performance of minimal-function devices through the application of line-shaped encoding with full CSIT and simple combining methods [2]–[10]. Notably, the STLC has demonstrated scalability to an arbitrary number of transmit antennas [2] and achievement of full spatial diversity in multiple-input multiple-output channels [11].

To reveal the fundamental performance of the STLC, notable studies have been conducted. In [12], the analysis focused on the ergodic capacity of the systems employing seven orthogonal STLCs. In [11], [13], error rates have been mathematically studied for the orthogonal STLC system with two receive antennas. Furthermore, through the error rate analysis in [14], the efficacy of quasi-orthogonal STLCs in achieving full spatial diversity has been established when a large number of transmit antennas are deployed. However, the aforementioned studies in [11], [13], [14] have been conducted under the presumption of utilizing quadrature amplitude modulation (QAM).

The performance of STLC systems has not been investigated under phase-shift keying (PSK) modulation despite the practicality of its employment [1], [15]. Hence, this study aims to reveal the theoretical performance of STLC systems when PSK modulation is applied. By using the moment-generating function (MGF) method, we derive mathematical expressions of the symbol error rate (SER) and bit error rate (BER). Subsequently, utilizing the derived BER, we study the asymptotic performance characteristics regarding the diversity gain and coding gain. We validate the accuracy of the analysis through numerical simulations and discuss the performance behavior for the modulation order and the number of transmit antennas.

This work was supported in part by the National Research Foundation of Korea(NRF) grant funded by the Korea government(MSIT) (No. NRF-2022R1G1A1010641) and by IITP grant funded by the Korea government(MSIT) (No.2021-0-00874, Development of Next Generation Wireless Access Technology Based on Space Time Line Code).

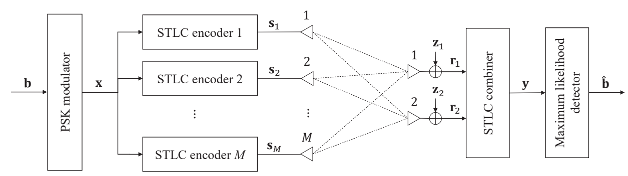

Fig. 1. $M \times 2$ STLC system model.

Notations: We use a lowercase boldface letter (e.g., $\mathbf{x}$) to denote a column vector. A superscript "$*$" denotes the complex conjugate operation for a complex scalar. For a random variable x, $\mathbb{E}[x]$ represents the statistical expectation of x, and $x \sim \mathcal{CN}\left(m, \sigma^2\right)$ indicates that x is a Gaussian random variable with mean m and variance σ^2.

II. STLC System Model

In Fig. 1, we illustrate an $M \times 2$ STLC system with M transmit antennas and two receive antennas, where M represents an arbitrary positive integer. In this configuration, we consider the transmitter to possess perfect knowledge of CSIT while the receiver has access to partial CSIR [1]. For $n \in \{1, 2\}$ and $m \in \{1, \ldots, M\}$, let $h_{n,m}$ be the channel gain between the mth transmit antenna and nth receive antenna. The channel gains $h_{n,m}$ follow a flat Rayleigh fading channel model, where each gain is a Gaussian random variable characterized by zero mean and unit variance, i.e., $h_{n,m} \sim \mathcal{CN}(0, 1)$. We define the sum of all individual channel gains, denoted by γ, as $\gamma = \sum_{m=1}^{M} (|h_{1,m}|^2 + |h_{2,m}|^2)$.

Let $\mathbf{b}$ be a binary sequence of length $2 \log_2 Q$, where Q represents the modulation order of a Gray-labeled PSK signal constellation $\mathcal{Q}$ (i.e., $Q = |\mathcal{Q}|$). These data bits $\mathbf{b}$

are modulated to form a PSK symbol vector $\mathbf{x} = [x_1, x_2]^{\mathrm{T}}$, where $\mathbb{E}[x_k] = \sigma_x^2$ holds for $k \in \{1, 2\}$. For the mth transmit antenna, a pair of modulated symbols is encoded into an STLC symbol vector of length two, denoted as $\mathbf{s}_m = [s_{m,1}, s_{m,2}]^{\mathrm{T}}$. Utilizing the available CSIT, the generation of two STLC symbols follows the process proposed in [1]:

$$s_{m,1} = \frac{1}{\sqrt{\gamma}} \left(h_{1,m}^* x_1 + h_{2,m}^* x_2^* \right), \tag{1a}$$

$$s_{m,2} = \frac{1}{\sqrt{\gamma}} \left(h_{2,m}^* x_1^* - h_{1,m}^* x_2 \right), \tag{1b}$$

where the normalization factor $1/\sqrt{\gamma}$ is determined to adhere to the transmit power constraint σ_x^2. Subsequently, the STLC symbols are transmitted in sequence via the mth transmit antenna at symbol time $t \in \{1, 2\}$.

For $n \in \{1, 2\}$, we define $\mathbf{r}_n = [r_{n,1}, r_{n,2}]^{\mathrm{T}}$ as the received STLC symbol vector via the nth receive antenna. At symbol time $t \in \{1, 2\}$, the tth component of the received STLC symbol vector is expressed as $r_{n,t} = \sum_{m=1}^{M} h_{n,m} s_{m,t} + z_{n,t}$, where $z_{n,t}$ is additive white Gaussian noise (AWGN) following a Gaussian distribution with mean zero and variance σ_z^2, i.e., $z_{n,t} \sim \mathcal{CN}\left(0, \sigma_z^2\right)$. With received symbols $\{r_{n,t}\}$, the receiver performs linear operations to generate a combined symbol vector, denoted as $\mathbf{y} = [y_1, y_2]^{\mathrm{T}}$, in which each component is calculated as follows [1]:

$$y_1 = r_{1,1} + r_{2,2}^* = \sqrt{\gamma} x_1 + z_{1,1} + z_{2,2}^*, \tag{2a}$$

$$y_2 = r_{2,1}^* - r_{1,2} = \sqrt{\gamma} x_2 + z_{2,1}^* - z_{1,2}. \tag{2b}$$

With the combined symbols, the receiver can employ the maximum likelihood (ML) detection to recover either the transmitted modulated symbols $\hat{\mathbf{x}}$ or the corresponding binary bits $\hat{\mathbf{b}}$.

III. Performance Analysis

From (2), we note that the effective channel gain is represented by $\sqrt{\gamma}$, while the effective noise variance takes the form of $2\sigma_z^2$. As a result, we can readily express the instantaneous signal-to-noise ratio (SNR) as

$$\xi = \frac{\gamma \sigma_x^2}{2\sigma_z^2} = \frac{\rho}{2} \gamma, \tag{3}$$

where ρ denotes the SNR of the single transmit and receive antenna system, i.e., $\rho = \sigma_x^2 / \sigma_z^2$. Upon observing (3), it is evident that ξ follows a scaled chi-squared distribution with $4M$ degrees of freedom. Consequently, the MGF of the instantaneous SNR can be expressed as follows [11]:

$$\Psi(t) = \mathbb{E}\left[e^{\xi t}\right] = \left(1 - \frac{\rho}{2} t\right)^{-2M}. \tag{4}$$

Symbol Error Rate (SER): For a given instantaneous SNR ξ in the STLC system applying the Q-ary PSK modulation, the conditional SER is given by [16]

$$P_{\mathrm{s}|\xi} = 2\Phi\left(\sqrt{2\xi} \sin\left(\frac{\pi}{Q}\right)\right), \tag{5}$$

where $\Phi(\cdot)$ represents the Gaussian Q-function, i.e., $\Phi(x) = \frac{1}{\sqrt{2\pi}} \int_x^\infty e^{-\frac{t^2}{2}} dt$ for $x \geq 0$. Utilizing the relation $\Phi(x) \approx \frac{1}{12} e^{-\frac{x^2}{2}} + \frac{1}{6} e^{-\frac{2x^2}{3}}$ [17], [18], the conditional SER can be approximated as

$$P_{\mathrm{s}|\xi} \approx \frac{1}{6} e^{-\xi \sin^2\left(\frac{\pi}{Q}\right)} + \frac{1}{3} e^{-\frac{4}{3}\xi \sin^2\left(\frac{\pi}{Q}\right)}. \tag{6}$$

Hence, by taking expectation with respect to ξ on both sides, we can obtain the approximated expression for the SER as

$$P_{\mathrm{s}} \approx \frac{1}{6} \Psi\left(-\sin^2\left(\frac{\pi}{Q}\right)\right) + \frac{1}{3} \Psi\left(-\frac{4}{3} \sin^2\left(\frac{\pi}{Q}\right)\right) \tag{7}$$

where $\Psi(\cdot)$ represents the MGF defined in (4).

Bit Error Rate (BER): When employing the Q-ary PSK modulation for the STLC system, the conditional BER is referred to as follows [19]:

$$P_{\mathrm{b}|\xi} = \frac{2}{\max(\log_2 Q, 2)} \sum_{i=1}^{\max(\frac{Q}{4}, 1)} \Phi\left(\sqrt{2\xi} \sin\left(\frac{(2i-1)\pi}{Q}\right)\right) \tag{8}$$

Following a similar approach, we approximate the Gaussian Q-function and then compute the expectation on both sides, resulting in (11), shown at the bottom of the page.

Diversity Gain and Coding Gain: To reveal the asymptotic performance, we deduce the diversity and coding gains of the STLC system. Under the assumption of a high ρ, (11) is approximated to (12), shown at the bottom of the page. Upon substituting (12) into the definition, the diversity gain is readily shown as

$$D = \lim_{\rho \to \infty} -\frac{\log_{10} P_{\mathrm{b}}}{\log_{10} \rho} = 2M. \tag{13}$$

Moreover, by employing the definition $G = \lim_{\rho \to \infty} \frac{(P_{\mathrm{b}})^{-1/D}}{\rho}$, we can derive the coding gain, as defined in (12).

$$P_{\mathrm{b}} \approx \frac{2}{\max(\log_2 Q, 2)} \sum_{i=1}^{\max(\frac{Q}{4}, 1)} \left[\frac{1}{12} \Psi\left(-\sin^2\left(\frac{(2i-1)\pi}{Q}\right)\right) + \frac{1}{6} \Psi\left(-\frac{4}{3} \sin^2\left(\frac{(2i-1)\pi}{Q}\right)\right)\right], \tag{11}$$

$$\approx \underbrace{\frac{2}{\max(\log_2 Q, 2)} \sum_{i=1}^{\max(\frac{Q}{4}, 1)} \left[\frac{1}{12} \left(\frac{1}{2} \sin^2\left(\frac{(2i-1)\pi}{Q}\right)\right)^{-2M} + \frac{1}{6} \left(\frac{2}{3} \sin^2\left(\frac{(2i-1)\pi}{Q}\right)\right)^{-2M}\right]}_{\triangleq G} \rho^{-2M} \tag{12}$$

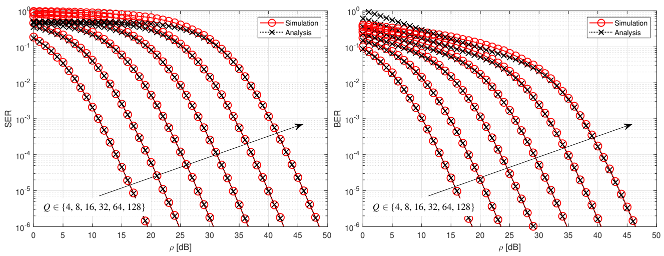

(a) SER (b) BER

Fig. 2. Performance of 2×2 STLC system with Q-ary PSK modulation ($Q \in \{4, 8, 16, 32, 64, 128\}$).

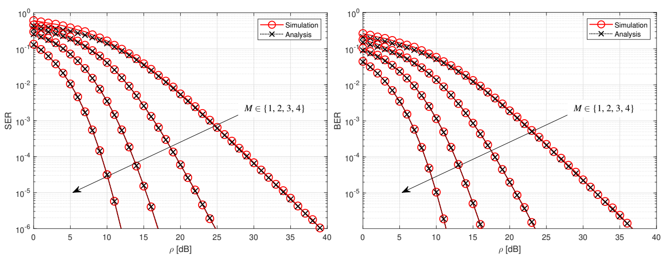

(a) SER (b) BER

Fig. 3. Performance of $M \times 2$ STLC system with 8-PSK modulation ($M \in \{1, 2, 3, 4\}$).

Through the analysis, we mathematically demonstrate that the diversity gain exhibits a proportional increase for the number of transmit antennas. It is particularly noteworthy that the STLC systems can achieve the full spatial diversity of $2M$. Moreover, we note that the coding gain increases for the number of transmit antennas while decreasing with respect to the modulation order.

IV. Simulation Results

Through Figs. 2 and 3, we validate the analysis in Section III, and discuss the performance of $M \times 2$ STLC systems with the Gray-labeled PSK modulation. Based on the simulations for diverse antenna configurations and modulation orders, the analytical results show good agreement with the Monte Carlo simulation results. Therefore, we can verify sufficient accuracy of the mathematical analysis in (7), (11), and (13).

Figure 2 shows the SER and BER of the STLC system with two transmit antennas ($M = 2$) when modulation orders are set to $Q \in \{4, 8, 16, 32, 64, 128\}$. Notably, the curves show identical slopes at high ρ, indicating the consistent preservation of the full spatial diversity gain, i.e., the order of $2M$, regardless of the modulation orders. Meanwhile, as the modulation order increases, degradation in error rates is observed due to the corresponding decrease in the coding gain.

In Fig. 3, we evaluate the SER and BER of the STLC systems using 8-PSK modulation ($Q = 8$) while varying the number of transmit antennas ($M \in \{1, 2, 3, 4\}$). As observed by increasing slopes of the curves, deploying more transmit antennas leads to substantial improvement in error rates. This improvement is attributed to the proportionally increased diversity gain and the increased coding gain.

V. Conclusion

In this study, we investigate the fundamental performance of the STLC systems employing the Gray-labeled PSK modulation. By exploiting the MGF of the instantaneous SNR, we conducted a mathematical analysis that comprehensively covered three aspects: 1) SER, 2) BER, and 3) diversity gain and coding gain. The analysis reveals that, with the application of PSK modulation, the STLC system can achieve full spatial diversity irrespective of the modulation order and the number of transmit antennas. Through the analysis and simulation, we noticed the guideline for the system design and highlighted the practical usefulness of the PSK modulation for the STLC systems.

References

[1] J. Joung, "Space–time line code," *IEEE Access*, vol. 6, pp. 1023–1041, Feb. 2018.

[2] ——, "Space–time line code for massive MIMO and multiuser systems with antenna allocation," *IEEE Access*, vol. 6, pp. 962–979, Feb. 2018.

[3] ——, "Energy efficient space–time line coded regenerative two-way relay under per-antenna power constraints," *IEEE Access*, vol. 6, pp. 47 026–47 035, Sep. 2018.

[4] J. Joung and J. Choi, "Space-time line codes with power allocation for regenerative two-way relay systems," *IEEE Trans. Veh. Technol.*, vol. 68, no. 5, pp. 4884–4893, May 2019.

[5] J. Joung, J. Choi, and B. C. Jung, "Double space–time line codes," *IEEE Trans. Veh. Technol.*, vol. 69, no. 2, pp. 2316–2321, Feb. 2020.

[6] J. Joung, "Random space–time line code with proportional fairness scheduling," *IEEE Access*, vol. 8, pp. 35 253–35 262, Feb. 2020.

[7] J. Seo, H. Jin, J. Joung, and B. C. Jung, "Uplink NOMA random access systems with space–time line code," *IEEE Trans. Veh. Technol.*, vol. 69, no. 4, pp. 4522–4526, Apr. 2020.

[8] H. Yu and J. Joung, "Frame structure design for vehicular-to-roadside unit communications using space–time line code under time-varying channels," *IEEE Syst. J.*, vol. 15, no. 2, pp. 3150–3153, Jun. 2021.

[9] J. Joung, H. Yu, and J. Zhao, "Bandwidth design for energy-efficient unmanned aerial vehicle using space–time line code," *IEEE Syst. J.*, vol. 15, no. 2, pp. 3154–3157, Jun. 2021.

[10] J. Choi, J. Joung, and B. C. Jung, "Space–time line code for enhancing physical layer security of multiuser MIMO uplink transmission," *IEEE Syst. J.*, vol. 15, no. 3, pp. 3336–3347, Sep. 2021.

[11] S.-C. Lim and J. Joung, "Transmit antenna selection for space–time line code systems," *IEEE Trans. Commun.*, vol. 69, no. 2, pp. 786–798, Feb. 2021.

[12] ——, "Ergodic capacity of space–time line code systems with transmit antenna selection," *IEEE Trans. Veh. Technol.*, vol. 71, no. 8, pp. 9089–9094, Aug. 2022.

[13] Y. Pang, Y. Xiao, X. Lei, and Y. Li, "Performance analysis and antenna selection for space time line code," *IEEE Access*, vol. 8, pp. 193 503–193 511, Nov. 2020.

[14] S.-C. Lim and J. Joung, "Full-rate space–time line code for four receive antennas," *IEEE Wireless Commun. Lett.*, vol. 11, no. 3, pp. 602–606, Mar. 2022.

[15] J. Joung and B. C. Jung, "Machine learning based blind decoding for space–time line code (STLC) systems," *IEEE Trans. Veh. Technol.*, vol. 68, no. 5, pp. 5154–5158, May 2019.

[16] J. G. Proakis, *Digital Communications*, 5th ed. McGraw Hill, 2007.

[17] N. Kim, Y. Lee, and H. Park, "Performance analysis of MIMO system with linear MMSE receiver," *IEEE Trans. Wireless Commun.*, vol. 7, no. 11, pp. 4474–4478, Nov. 2008.

[18] S.-C. Lim, N. Kim, and H. Park, "Uplink SCMA system with multiple antennas," *IEEE Trans. Veh. Technol.*, vol. 66, no. 8, pp. 6982–6992, Aug. 2017.

[19] J. Lu, K. B. Letaief, J. C.-. Chuang, and M. L. Liou, "M-PSK and M-QAM BER computation using signal-space concepts," *IEEE Trans. Commun.*, vol. 47, no. 2, pp. 181–184, Feb. 1999.